Supplementary Information

Insights into the binding behavior of native and non-native cytochromes to Photosystem I from *Thermosynechococcus elongatus*

Adrian Kölsch[1*], Mahdi Hejazi[1], Kai R. Stieger[2], Sven C. Feifel[2], Jan F. Kern[3], Frank Müh[4], Fred Lisdat[2], Heiko Lokstein[5], Athina Zouni[1*]

[1]Humboldt-Universität zu Berlin, Institute for Biology, Biophysics of Photosynthesis, Philippstr. 13, 10115 Berlin, Germany
[2]University of Applied Sciences Wildau, Institute for Applied Life Sciences, Biosystems Technology, Hochschulring 1, 15745 Wildau, Germany
[3]Lawrence Berkeley National Laboratory, 1 Cyclotron Road, CA 94720 Berkeley, USA
[4]Johannes Kepler University Linz, Institute for Theoretical Physics, Department of Theoretical Biophysics, Altenberger Str. 69, 4040 Linz, Austria
[5]Charles University, Department of Chemical Physics and Optics, Ke Karlovu 3, CZ-121 16 Praha 2, Czech Republic

*To whom correspondence should be addressed: A. Kölsch and Prof. A. Zouni, Humboldt-Universität zu Berlin, Institute for Biology, Biophysics of Photosynthesis, Philippstr. 13, 10115 Berlin, Germany. Telephone: +49 30209347930; FAX: +49 30209347934; E-mail: koelscha@hu-berlin.de and athina.zouni@hu-berlin.de

Table S1

MALDI-MS analysis of purified PS I. Following purification and crystallization, PS I crystals were dissolved in 5 mM MES-NaOH, pH 6.0 and 30 mM $MgSO_4$. MS spectra were recorded in linear mode. The standard deviation is given for 12 independent PS I preparations.

	PsaM	PsaX	PsaI	PsaJ	PsaE	PsaK	PsaC	PsaF	PsaD	PsaL
Calculated mass* (Da)	3424	4101	4166	4767	8389	8480	8800	15113	15370	16251
Determined mass (Da)	3424 ±2	3970 ±2	4195 ±2	4796 ±2	8261 ±3	8392 ±3	8672 ±3	15116 ±7	15232 ±12	16125 ±9

*Post translational modifications are described in (1).

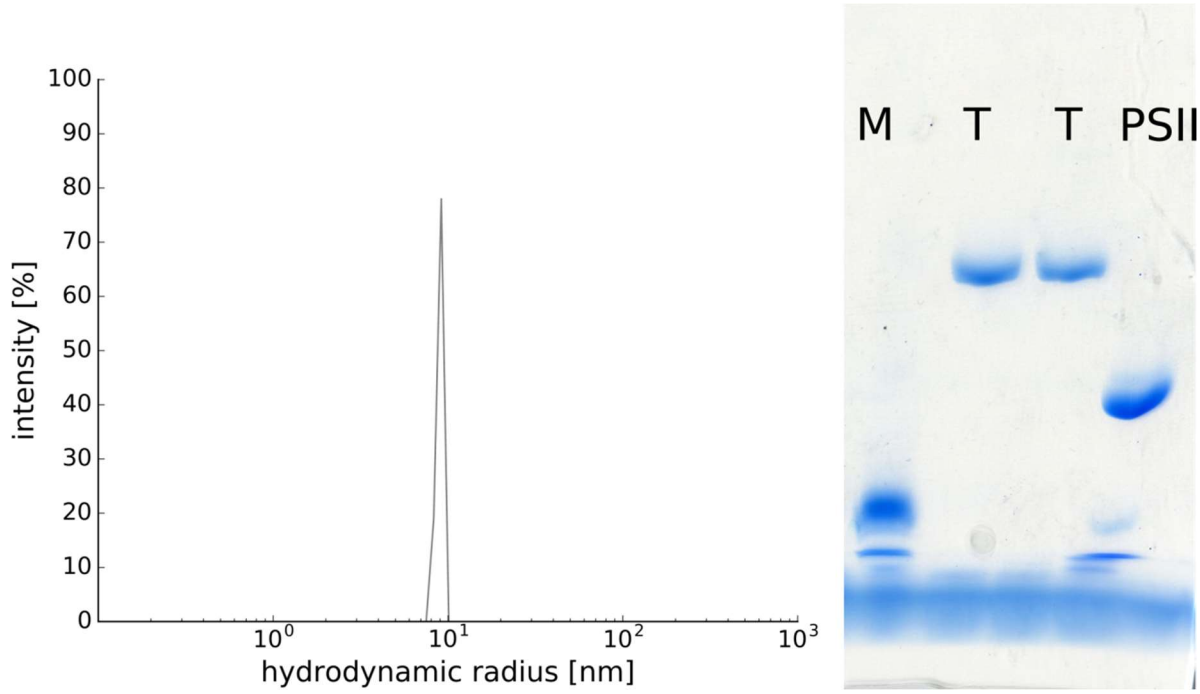

Figure S1: Hydrodynamic radius of trimeric PS I measured by dynamic light scattering (DLS, left) and blue native (BN) PAGE of trimeric PS I (T, 1000 kDa) in comparison to monomeric PS I (M, 340 kDa) and dimeric photosystem II (PSII, 750 kDa) (right). For DLS, PS I crystals were dissolved in 100 mM NaCl, 0.02 % DDM and 25 mM Tricine-NaOH, pH 8 to 5 µM P_{700} and filtered through a 0.2 µm filter. For BN-PAGE, PS I crystals corresponding to 5 µg of chlorophyll were dissolved in BN-solubilisation buffer containing 0.2 % DDM and applied to a gradient gel containing 3 to 9 % polyacrylamide.

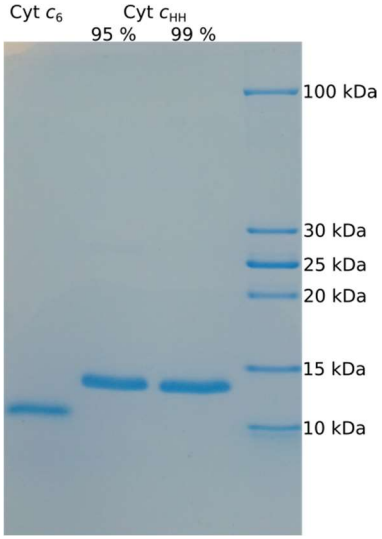

Figure S2: SDS-PAGE of purified cyt c_6 and cyt c_{HH} at ≥ 95 % and ≥ 99 % purity, obtained from Sigma Aldrich (Germany). Homogeneity of the proteins was analyzed according to the protocol of Laemmli (2). Samples were denatured in sample buffer at 95 °C for 5 min and applied to a 15 % poly-acryl-amide gel.

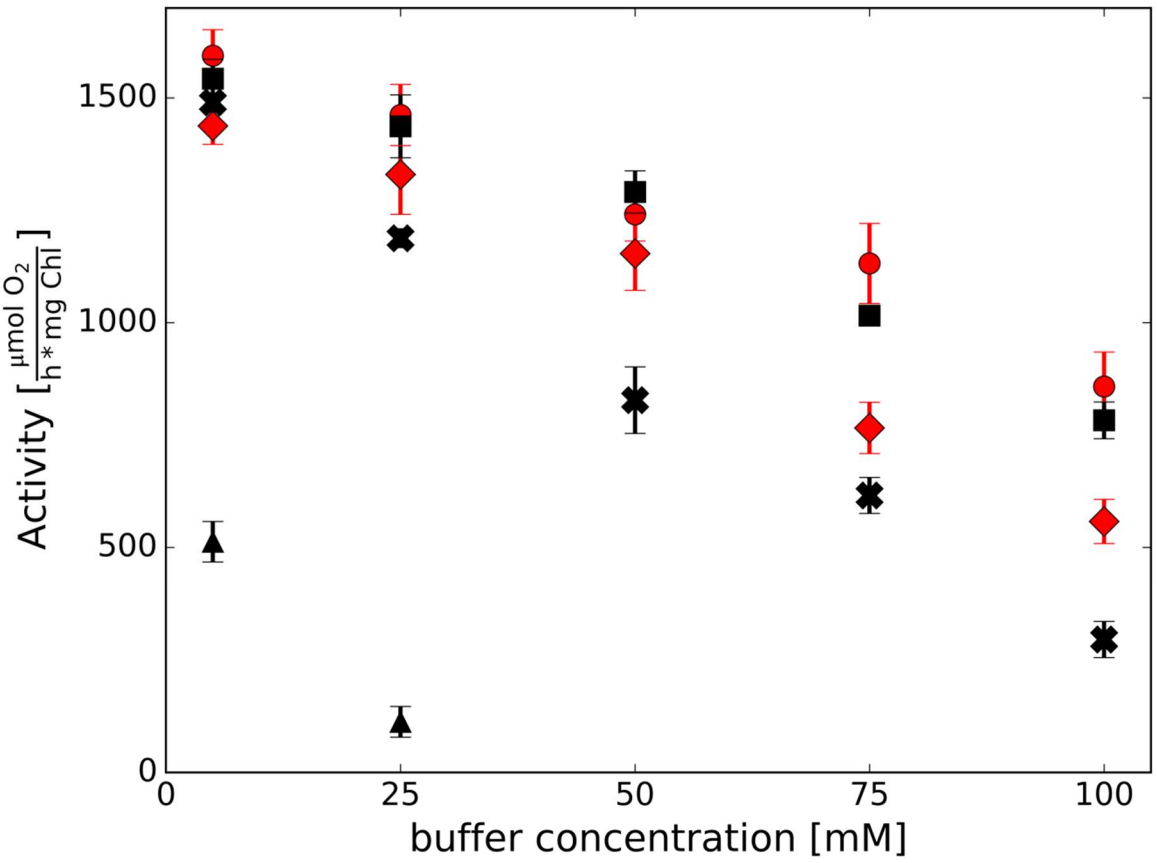

Figure S3: PS I - cyt c_{HH} oxygen reduction activity as a function of the buffer concentration. The activity was highest in Tricine (red circles) and Tris (black squares) buffer, while it was lower in HEPES (red diamond), MOPS (black cross) and phosphate buffer (black triangles) at pH 8 with 16 µM cyt c_{HH}. Standard deviations result from three independent measurements.

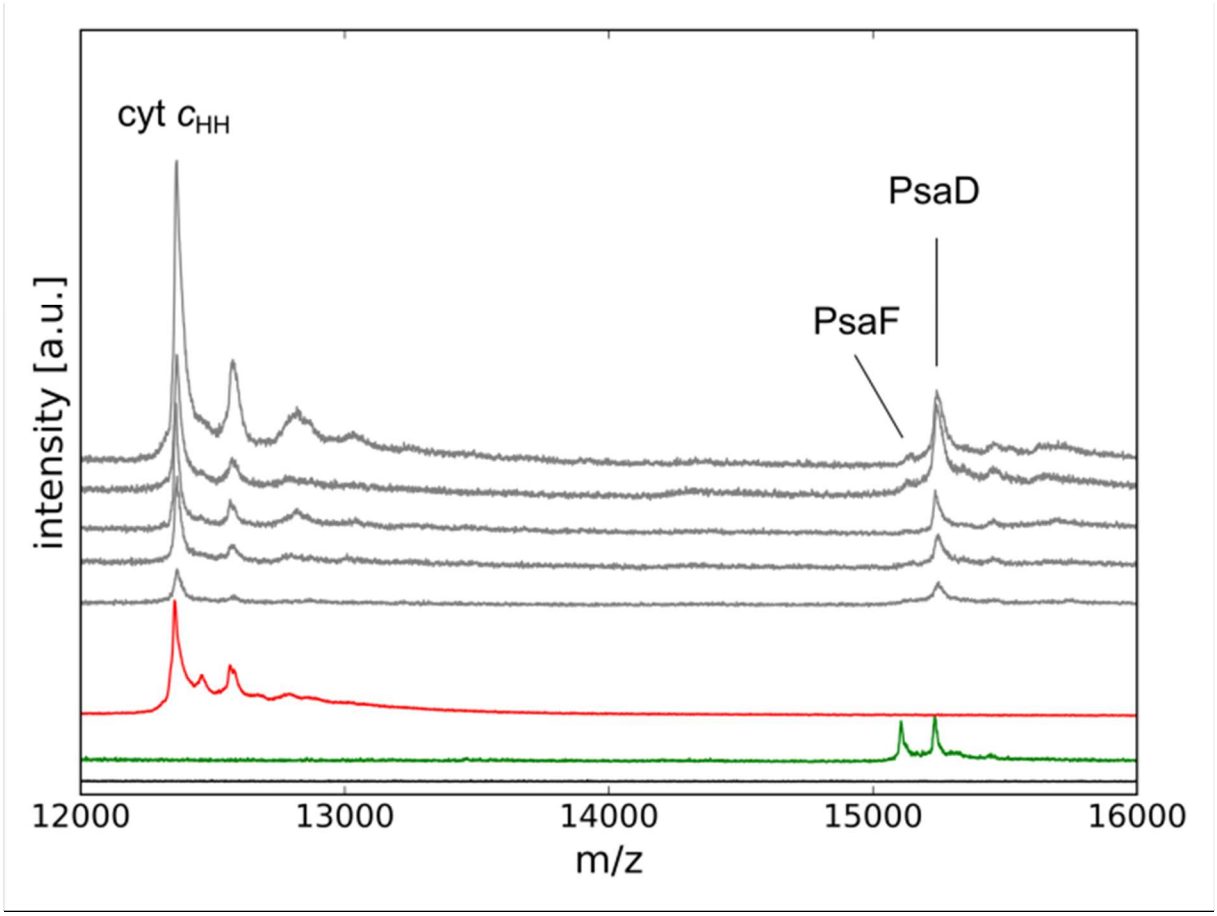

Figure S4. Section of MALDI-TOF analysis of single PS I - cyt c_{HH} co-crystals grown in 5 independent batches (grey spectra). For comparison, spectra of cyt c_{HH} (95 % purity) and PS I are shown in red and green, respectively. Crystals were washed six times prior to analysis to avoid contamination by free cyt c_{HH}. Neither cyt c_{HH} nor PS I are present in the supernatant from the last washing step (black spectrum).

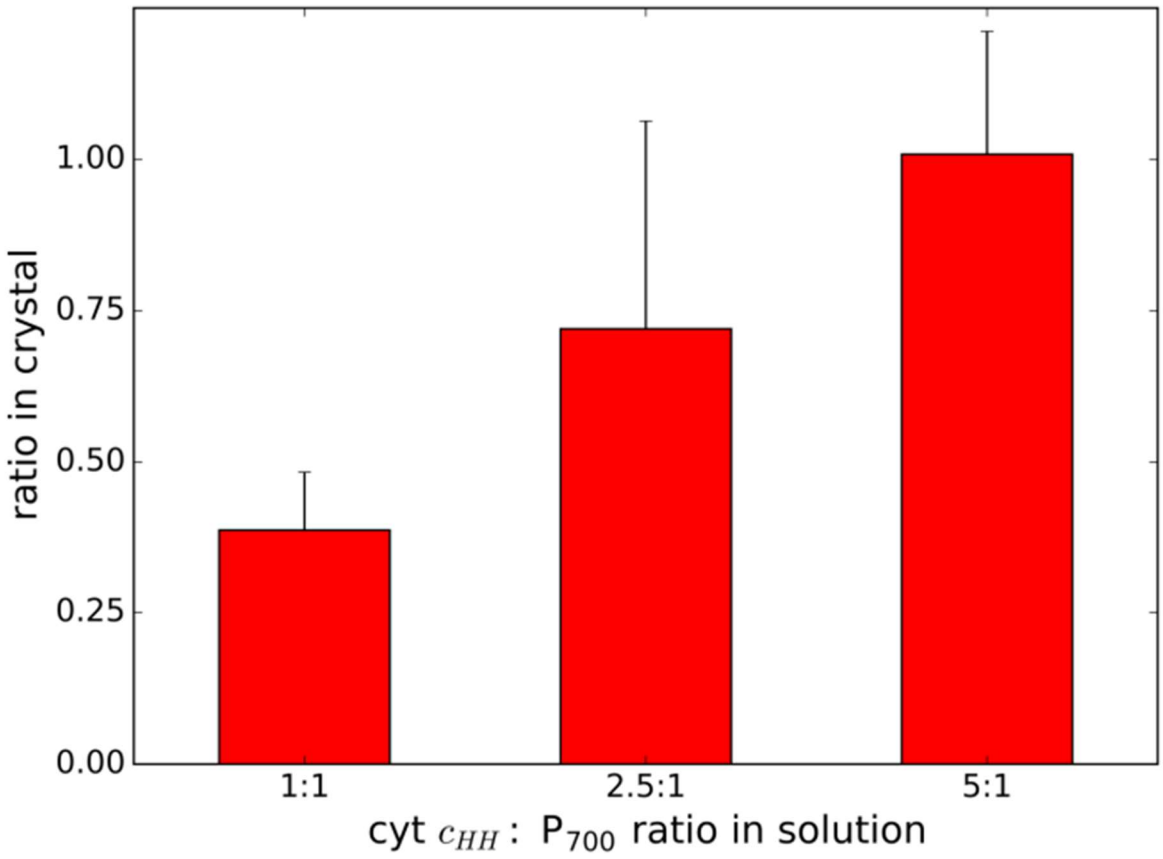

Figure S5. Ratio of cyt c_{HH} to P_{700} in PS I-cyt c_{HH} co-crystals. Batches of crystals were washed, dissolved and cyt c_{HH} was separated from PS I for photometric quantification. Standard deviations result from three to twelve independent measurements.

Table S2

X-ray data collection and refinement statistics. Values in parenthesis are for the high resolution shell.

Statistics	Values
Wavelength (Å)	0.999
Space Group	$P6_3$
Cell Dimensions	
a, b, c (Å)	281.4, 281.4, 165.6
α, β, γ (°)	90, 90, 120
Resolution (Å)	47.36 – 3.42 (3.63 - 3.42)
Multiplicity	15.88
I/σI	8.79 (1.75)
R_{meas}	0.42 (1.60)
Completeness (%)	99.2 (97.0)
No. of reflections	99609
R_{work}/R_{free}	0.2611/0.3169
Rmsd Bond lengths (Å)	0.0162
Rmsd Bond angles (°)	5.8874

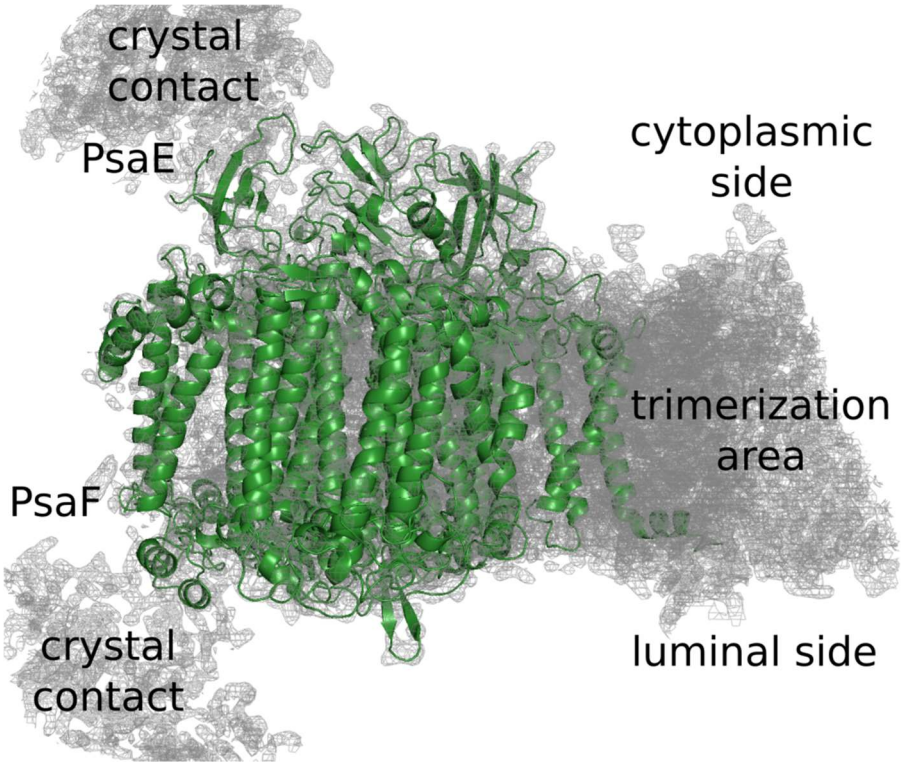

Figure S6: Electron density map (grey) of a PS I – cyt c_{HH} co-crystal at 3.4 Å resolution with the respective PS I model (green) at 2 σ contour level. Crystal contacts are formed between PsaE on the cytoplasmic side and PsaF on the luminal side of PS I. All electron density can be assigned to PS I, and no density is found for cyt c_{HH}.

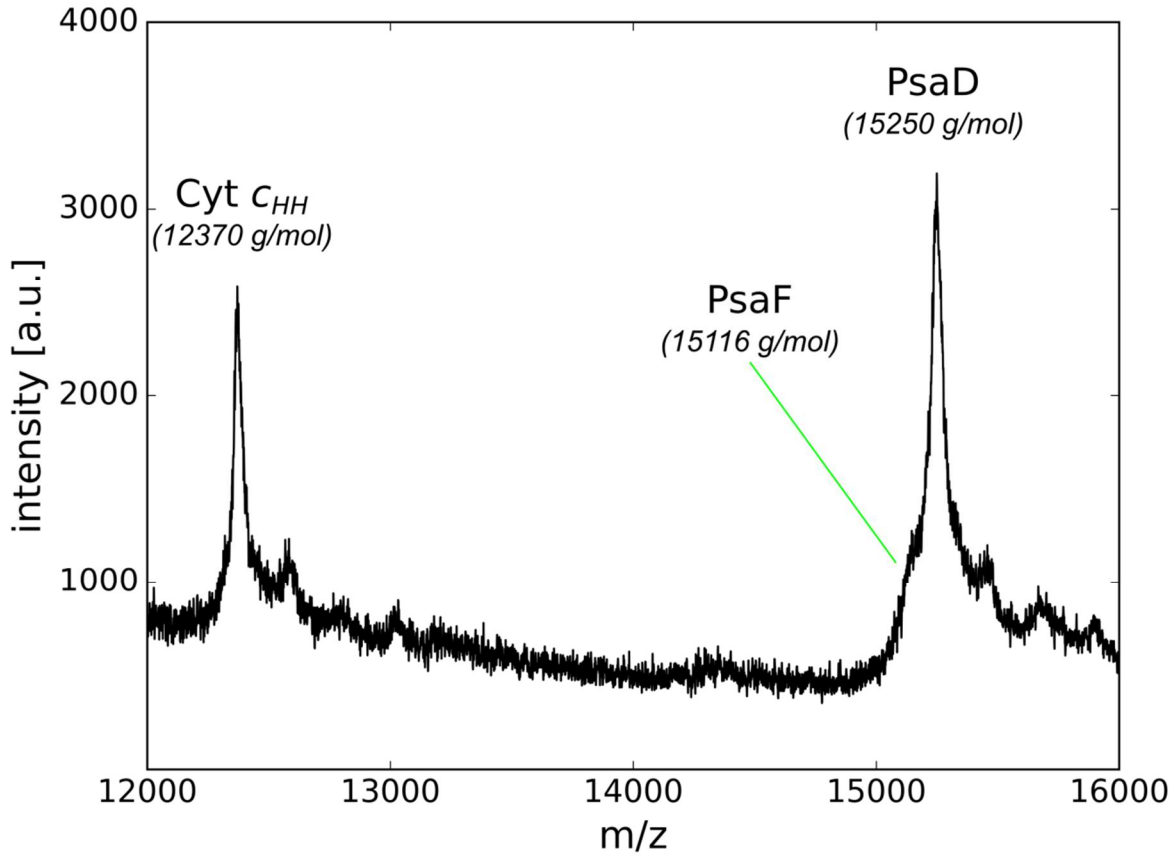

Figure S7: MALDI-TOF analysis of a single PS I cyt c_{HH} co-crystal after structure analysis at BESSY II at 3.5 Å resolution. The cyt c_{HH} peak is clearly visible, while not all subunits were found by MALDI-TOF, although they were present in the electron density map (e.g. PsaF).

Table S3: Solubility of PS I at high protein concentration and low salt concentration. PS I crystals were dissolved in Tricine pH 8.0 buffer containing 0.02 % DDM and 100 mM NaCl. The solution was slowly diluted to 30 µM P_{700} and its final NaCl concentration. The solution was filtered into a disposable cuvette and measured by dynamic light scattering. A high polydispersity (Pd) results from protein aggregation, while a low Pd indicates monodisperse proteins. Standard deviations result from three independent measurements.

NaCl [mM]	Pd at 30 µM P_{700} [%]
10	-
15	18 ± 3
20	10 ± 1
25	5 ± 1
30	5 ± 1
35	5 ± 1

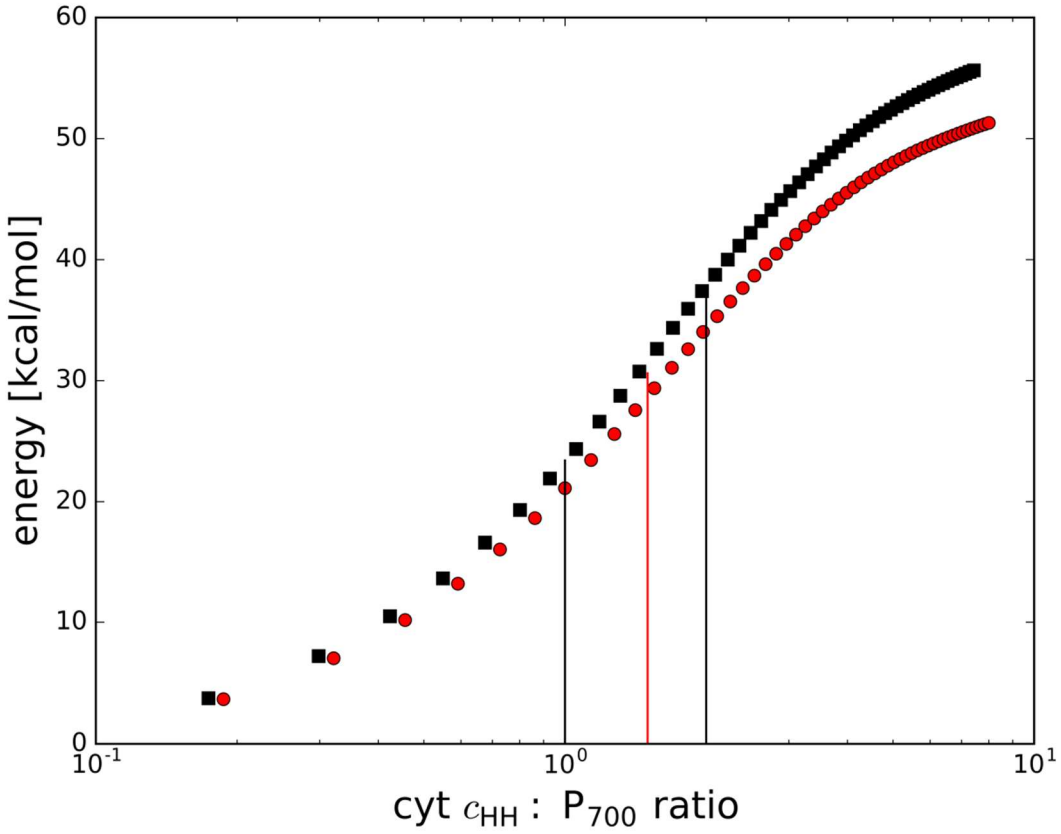

Fig. S8: ITC data from Fig. 4 in semilogarithmic representation. Shown is the summed energy of the titrations against the cyt c_{HH} : P_{700} ratio for measurements in oxidized (black squares) and reduced (red circles) conditions. The black vertical bars represent a ratio of 1 and 2, while the red bar represents the ratio of 1.5, which was calculated to be the number of binding sites by a model for one set of binding sites (Table 2).

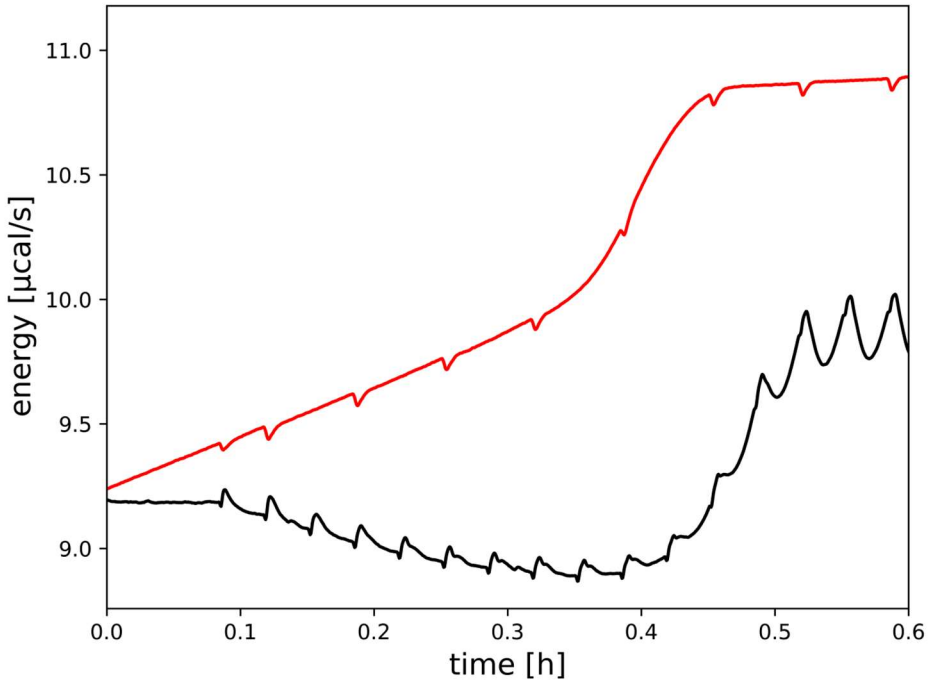

Figure S9: Isothermal titration calorimetry of PS I with cyt c_6. Thermogram for exemplary measurements with oxidized (black) and reduced (red) proteins. Measurements were performed at 20 °C in 25 mM Tricine buffer, pH 8.0 with 200 mM $MgSO_4$ and 0.02 % DDM. Each titration step consisted of 5 µl injected volume from 1 mM cyt c_6 in 50 µM P_{700}. Measurements under reducing conditions were performed in the presence of 5 mM ascorbic acid and measurements under oxidizing conditions in the absence or presence of up to 15 mM $K_3(CN)_6Fe(III)$. A strong baseline shift appeared in all measurements under these conditions, indicating the presence of a reaction that cannot be described by a simple binding enthalpy model.

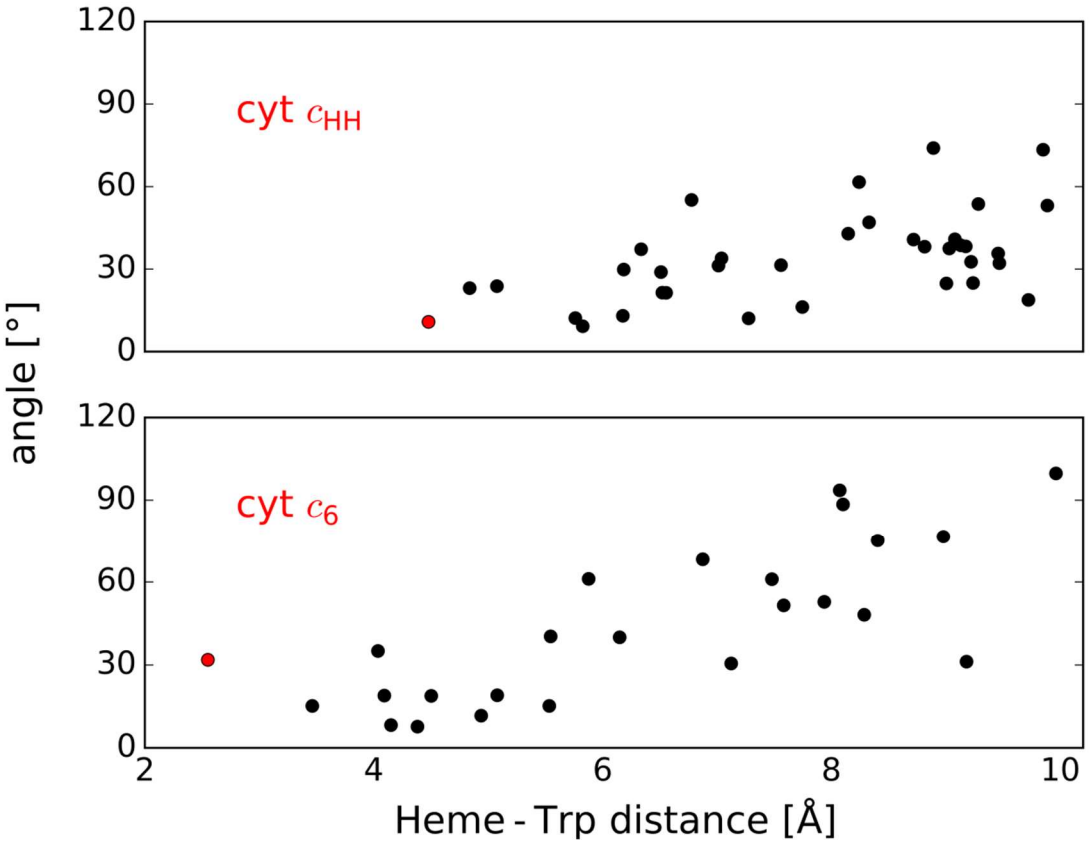

Figure S10: Cyt c_{HH} (top) and cyt c_6 (bottom) can bind at the P_{700}-docking site in different orientations. The depicted docking states have less than 10 Å C-C distance between the heme group and the luminal tryptophan residues W(A655) and W(B632) and more than -15 kcal/mol binding energy. The angle was calculated between two lines, formed by the geometrical center of the cytochrome (g) with the iron from the heme group and by g with the Mg-ions of P_{700}. The docking states shown in Figure 6 are highlighted in red.

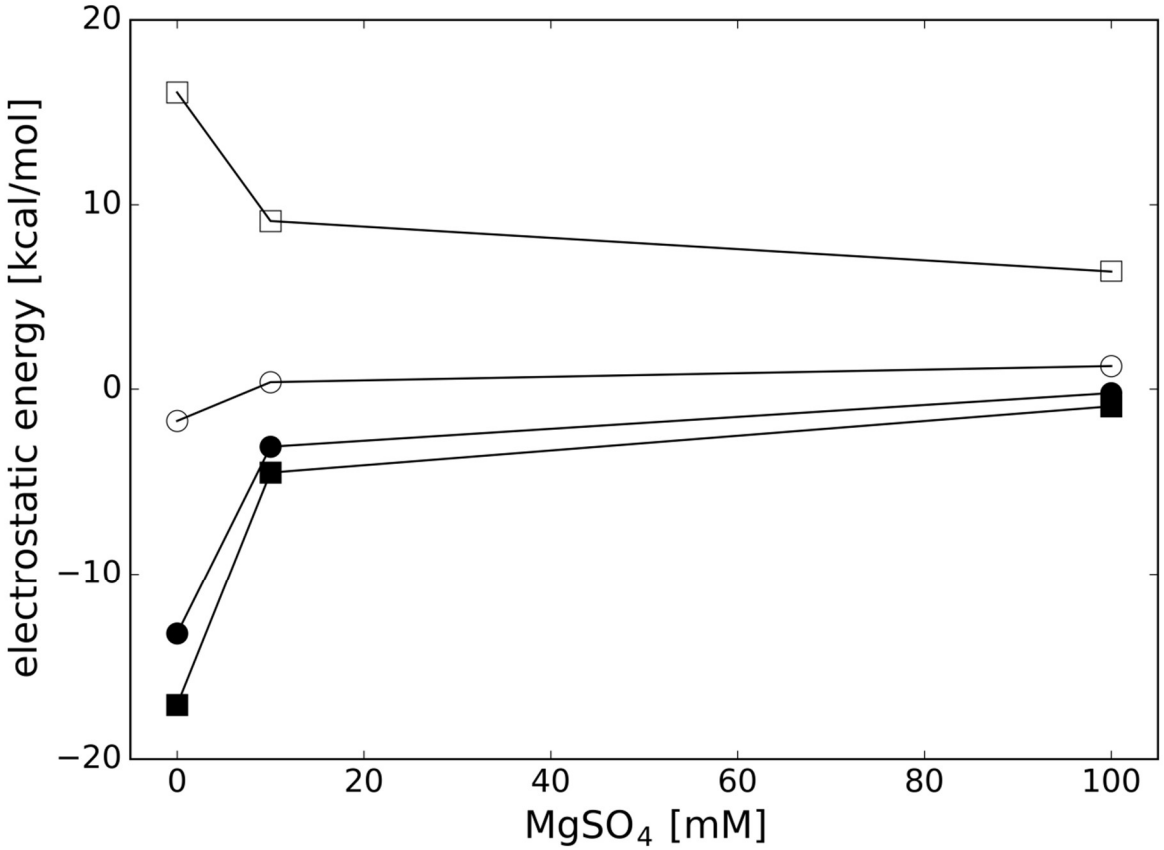

Figure S11: Re-calculation of electrostatic energy of the docking sites shown in Figure 6. Cyt c_{HH} (filled symbols) and cyt c_6 (open symbols) were calculated at pH 6 (circles) and pH 8 (squares) in the presence of 0, 10 and 100 mM $MgSO_4$ by using the Poisson-Boltzmann equation. The protein dielectric constant was set to 10, and the temperature to 20 °C. For cyt c_6 a 6x His-tag with random conformation was added to the protein-structure. Calculations performed by the adaptive Poisson-Boltzmann solver (APBS 1.4) with amber force field.

Table S4

Distance between cyt c_6 and PS I residues derived from the docking site shown in Figure 6.

Residue cyt c_6	Residue PS I	Distance [Å]	expected perturbation *
ARG64	PsaB GLN636	1.5	significant
MET26	PsaA ILE634	2.2	not homolog
MET19	PsaA ASN638	2.2	significant
ALA16	PsaA ARG651	2.3	not homolog
ALA57	PsaA SER659	2.4	significant
VAL25	PsaA ARG750	2.4	strong
GLY12	PsaB ASN639	2.5	significant
HEM88	PsaA TRP655	2.5	
SER11	PsaB ASN642	2.6	strong
ASN13	PsaB GLN636	2.6	strong
GLY20	PsaB PHE644	2.6	not significant
GLY63	PsaB LYS738	2.7	not significant
LEU65	PsaB GLN636	2.8	significant
VAL24	PsaA ASP652	2.9	strong
ALA27	PsaA ILE634	3.0	strong
ALA15	PsaB PHE644	3.0	significant
CYS17	PsaA TRP655	3.0	significant
PRO59	PsaA TRP655	3.2	not significant
PHE61	PsaB GLN636	3.3	strong
ASN23	PsaA THR635	3.4	significant

*NMR signals of cyt c_6 amino acids from *Nostoc* sp. PCC 7119 which were perturbed after addition of PS I (3).

Table S5

Distance between cyt c_{HH} and PS I residues derived from the docking site shown in Figure 6.

Residue cyt c_{HH}	Residue PS I	Distance [Å]
THR28	PsaB TRP631	2.6
LYS25	PsaA ILE634	2.7
ILE81	PsaB GLN636	2.7
GLN16	PsaA ARG651	3.0
HEM105	PsaB SER635	3.3
GLN12	PsaB PHE644	3.3
PHE82	PsaB GLN636	3.5
LYS72	PsaB GLN636	3.5
GLY77	PsaB GLU609	3.7
LYS79	PsaB LEU632	3.8
ALA83	PsaB GLN636	4.0
PRO76	PsaB GLU609	4.1
LYS27	PsaA GLN660	4.6
VAL11	PsaB PHE644	4.8
CYS17	PsaA TRP655	4.9
HIS26	PsaA GLN660	5.3
THR49	PsaB ASN611	5.4
ASP50	PsaF LYS16	5.6
THR78	PsaB GLU609	5.7
ALA51	PsaB ASN611	5.7

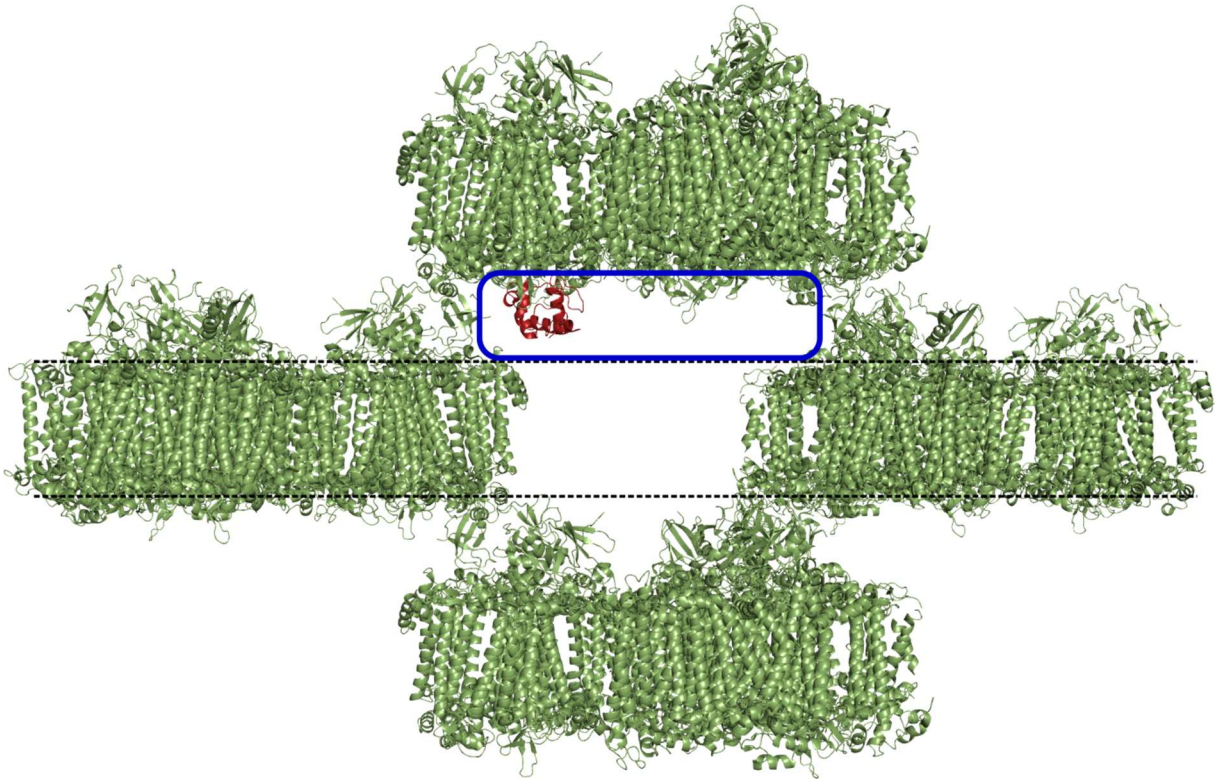

Figure S12: Photosystem I crystal lattice (green). The dotted lines mark the area where the DDM detergent belt may be localized. The remaining area where cyt c_{HH} could be positioned is highlighted by the blue box. A random docking state with cyt c_{HH} being close to P_{700} is inserted into the crystal lattice (red). Since there are no clashes of the docked cyt c_{HH} with neighboring PS I monomers, the lattice of a co-crystal does not need to be altered as compared to the PS I crystal lattice. The lattice was visualized by using the symexp command from PyMOL, with the crystal structure PDB-ID: 1jb0 (4).

Supplemental References

1. El-Mohsnawy, E., Kopczak, M. J., Schlodder, E., Nowaczyk, M., Meyer, H. E., Warscheid, B., Karapetyan, N. V., and Rögner, M. (2010) Structure and Function of Intact Photosystem 1 Monomers from the Cyanobacterium *Thermosynechococcus elongatus*. *Biochemistry*. **49**, 4740–4751
2. Laemmli, U. K. (1970) Cleavage of Structural Proteins during the Assembly of the Head of Bacteriophage T4. *Nature*. **227**, 680–685
3. Díaz-Moreno, I., Díaz-Quintana, A., Molina-Heredia, F. P., Nieto, P. M., Hansson, Ö., De la Rosa, M. A., and Karlsson, B. G. (2005) NMR Analysis of the Transient Complex between Membrane Photosystem I and Soluble Cytochrome c_6. *J. Biol. Chem.* **280**, 7925–7931
4. Jordan, P., Fromme, P., Witt, H. T., Klukas, O., Saenger, W., and Krauß, N. (2001) Three-dimensional structure of cyanobacterial photosystem I at 2.5 Å resolution. *Nature*. **411**, 909–917